



Article

Recombinant Integrin $\beta 1$ Signal Peptide Blocks Gliosis Induced by $A\beta$ Oligomers

Carolina Ortiz-Sanz^{1,2}, Francisco Llavero¹ , Jone Zuazo-Ibarra^{1,2}, Uxue Balantzategi^{1,2},
Tania Quintela-López^{1,2}, Ane Wyssenbach^{1,2}, Estibaliz Capetillo-Zarate^{1,2,3} , Carlos Matute^{1,2} ,
Elena Alberdi^{1,2,*} and José L. Zugaza^{1,3,4,*}

¹ Achucarro Basque Center for Neuroscience, Science Park of the UPV/EHU, Sede Building, 3rd Floor, Barrio de Sarriena s/n, 48940 Leioa, Spain; carolinaortizsan@gmail.com (C.O.-S.); francisco.llavero@ehu.eus (F.L.); jzuazoibarra@gmail.com (J.Z.-I.); uxue.balantzategi@ehu.eus (U.B.); t.lopez@ucl.ac.uk (T.Q.-L.); ane.wyssenbach@gmail.com (A.W.); estibaliz.capetillo@ehu.eus (E.C.-Z.); carlos.matute@ehu.eus (C.M.)

² Department of Neurosciences, Faculty of Medicine and Nursery UPV/EHU and CIBERNED, Barrio de Sarriena s/n, 48940 Leioa, Spain

³ IKERBASQUE, Basque Foundation for Science, Plaza Euskadi 5, 48009 Bilbao, Spain

⁴ Department of Genetics, Physical Anthropology and Animal Physiology, Faculty of Science and Technology, UPV/EHU, Barrio de Sarriena s/n, 48940 Leioa, Spain

* Correspondence: elena.alberdi@ehu.eus (E.A.); joseluis.zugaza@ehu.es (J.L.Z.)



Citation: Ortiz-Sanz, C.; Llavero, F.; Zuazo-Ibarra, J.; Balantzategi, U.; Quintela-López, T.; Wyssenbach, A.; Capetillo-Zarate, E.; Matute, C.; Alberdi, E.; Zugaza, J.L. Recombinant Integrin $\beta 1$ Signal Peptide Blocks Gliosis Induced by $A\beta$ Oligomers. *Int. J. Mol. Sci.* **2022**, *23*, 5747. <https://doi.org/10.3390/ijms23105747>

Academic Editors: Cristina Cereda, Carlo Morasso and Stella Gagliardi

Received: 29 April 2022

Accepted: 19 May 2022

Published: 20 May 2022

Publisher's Note: MDPI stays neutral with regard to jurisdictional claims in published maps and institutional affiliations.



Copyright: © 2022 by the authors. Licensee MDPI, Basel, Switzerland. This article is an open access article distributed under the terms and conditions of the Creative Commons Attribution (CC BY) license (<https://creativecommons.org/licenses/by/4.0/>).

Abstract: Glial cells participate actively in the early cognitive decline in Alzheimer's disease (AD) pathology. In fact, recent studies have found molecular and functional abnormalities in astrocytes and microglia in both animal models and brains of patients suffering from this pathology. In this regard, reactive gliosis intimately associated with amyloid plaques has become a pathological hallmark of AD. A recent study from our laboratory reports that astrocyte reactivity is caused by a direct interaction between amyloid beta ($A\beta$) oligomers and integrin $\beta 1$. Here, we have generated four recombinant peptides including the extracellular domain of integrin $\beta 1$, and evaluated their capacity both to bind in vitro to $A\beta$ oligomers and to prevent in vivo $A\beta$ oligomer-induced gliosis and endoplasmic reticulum stress. We have identified the minimal region of integrin $\beta 1$ that binds to $A\beta$ oligomers. This region is called signal peptide and corresponds to the first 20 amino acids of the integrin $\beta 1$ N-terminal domain. This recombinant integrin $\beta 1$ signal peptide prevented $A\beta$ oligomer-induced ROS generation in primary astrocyte cultures. Furthermore, we carried out intrahippocampal injection in adult mice of recombinant integrin $\beta 1$ signal peptide combined with or without $A\beta$ oligomers and we evaluated by immunohistochemistry both astrogliosis and microgliosis as well as endoplasmic reticulum stress. The results show that recombinant integrin $\beta 1$ signal peptide precluded both astrogliosis and microgliosis and endoplasmic reticulum stress mediated by $A\beta$ oligomers in vivo. We have developed a molecular tool that blocks the activation of the molecular cascade that mediates gliosis via $A\beta$ oligomer/integrin $\beta 1$ signaling.

Keywords: $A\beta$ oligomers; integrin $\beta 1$; interactive region; astrogliosis; microgliosis; interferent peptides

1. Introduction

Alzheimer's disease (AD) is the most common form of dementia and the most prevalent neurodegenerative disease [1]. Given that the first description made by Alois Alzheimer about pre-senile dementia refers to the formation of senile amyloid plaques and neurofibrillary tangles (aggregates of hyperphosphorylated tau protein) these elements are key pathological hallmarks of AD [2–7]. The formation of neurofibrillary tangles follows well-established patterns, while senile plaques appear and distribute in a random manner. The predictable alteration in the pattern and severity of the pathology permits the distinction of initial, intermediate and advanced stages based on investigations carried out by Braak

and Braak [7]. In addition to plaque distribution, the detection of amyloid β ($A\beta$) as a main constituent of the plaques [8] and the identification of gene mutations related to $A\beta$ synthesis in familial AD have led to formulating the amyloid cascade hypothesis [9,10], which postulates that $A\beta$ deposition in the extracellular space leads to neurodegeneration and subsequent cognitive impairment [11–13]. This hypothesis is not only supported by autosomal-dominant Alzheimer's disease (ADAD) but also an increase in the copy number of APP (e.g., triplication) is sufficient to cause AD and other amyloidosis [14]. However, the early CNS inflammation that aggravates the disease starts decades before the onset of AD, and it is characterized by neuronal and microglia-derived cytokines and chemokines, as well as mobilization of microglia toward $A\beta$ -laden neurons [15].

$A\beta$ peptide oligomers have been isolated from both animal models of AD [16,17] and cerebrospinal fluid (CSF) or brains from AD patients [18], in whom the presence of this peptide seems to correlate with the progression of the disease [19]. At nanomolar concentrations, $A\beta$ oligomers are able to induce neuronal death in hippocampal organotypic slices [20,21], but also to inhibit long-term potentiation [21,22], and to promote abnormal Ca^{2+} fluxes as well as cell membrane disruption [20,23]. The biochemical and structural complexity of $A\beta$ peptides make them very promiscuous molecules able to transduce signals through a repertoire of several receptors and proteins localized at the plasma membrane level both in neurons and in other cell types including glial cells [24,25].

Within the wide variety of effector molecules that interact with $A\beta$ peptides, integrins have emerged as key molecules in the development of AD [25] by regulating synaptic dysfunction, diversity of plasticity and long-term potentiation in the early stages of neurodegenerative diseases [26]. Alpha v integrins mediate $A\beta$ -induced inhibition of long-term potentiation [26]. Integrins are a complex family of glycoprotein receptors expressed ubiquitously [27,28]. In turn, they are a class of cellular adhesion molecules with adhesive and signal transduction functions [29,30] that drive to vital cellular events such as cell adhesion, differentiation or migration [31]. From a structural point of view, integrins are heterodimers constituted by alpha (α) and beta (β) subunits and bind non-covalently to mediate cell–cell and cell–extracellular matrix interactions. Each integrin recognizes specific ligands, which are either molecules of the extracellular matrix (ECM) (e.g., laminin and fibronectin) or other cell surface counter-receptors of the immunoglobulin superfamily (e.g., intracellular adhesion molecule-1 (ICAM-1)). However, integrins also have functional relationships with other membrane receptors such as ion channels including NMDA receptors and growth factor receptors [32].

During integrin activation, these glycoproteins change configuration from an inactive into an active form (stable extended high-affinity conformation) [33]. The active form triggers intracellular signaling cascades that are important for relaying information from the external environment to the inside of the cell. One of them is related to clustering between integrin and focal adhesions, leading to the assembly of numerous integrin-associated molecules such as talin, vinculin, paxillin, focal adhesion kinase (FAK), Src and integrin-linked kinase (ILK), that initiate canonical signaling pathways involving small GTPases of the Ras superfamily, ERK, JNK or AKT [34]. The heterodimers $\alpha 2\beta 1$, $\alpha 5\beta 1$, $\alpha v\beta 1$ and $\alpha v\beta 3$ can facilitate the deposition of $A\beta$ and induce neurotoxicity, which results in neuronal loss [35–37]. However, the molecular mechanisms by which integrins participate in the development of AD are still unknown.

Here, we have mapped the extracellular region of integrin $\beta 1$ in order to identify which domain binds to $A\beta$ oligomers. Using an *in vitro* binding assay, we have revealed that $A\beta$ oligomers bind to integrin $\beta 1$ signal peptide localized at the first 20 amino acids (aa) at the N-terminal (hereinafter referred as R_s). Application of this recombinant peptide in primary cultures of astrocytes inhibits ROS generation by $A\beta$ oligomers. Moreover, we have analyzed *in vivo* the effects of the R_s peptide in $A\beta$ oligomer-mediated astrogliosis and microgliosis, and in endoplasmic reticulum stress by performing intrahippocampal injections in mice. The findings reveal that integrin $\beta 1$ signal peptide, R_s , prevents gliosis and endoplasmic reticulum stress induced by $A\beta$ oligomers in mouse hippocampus. Together,

these data show that R_s peptide diminish A β oligomer-induced gliosis by interfering with integrin β 1 signaling.

2. Results

2.1. Integrin β 1 Signal Peptide Specifically Binds to A β Oligomers

First, we analyzed the amino acid sequence of integrin β 1 and selected four regions from its extracellular domain. The first region was constituted by the first 20 amino acids (aa) and it was identified as R_s, the second one, R_w, included up to aa 139, the third region covered aa 1 to 378 including the VWA domain (R_d), and the last region included the whole extracellular domain (from aa 1 to 728, R_t) (Figure 1A). Now, to determine what amino acid stretch could represent an effective binding domain for A β oligomers, four recombinant GST fusion proteins were generated (R_s, R_d, R_w, and R_t, fused to the GST protein), and their binding capacities to A β oligomers were determined by affinity chromatography as described in the Experimental procedures section. As shown in Figure 1B, the four fused proteins bound not only to the monomeric A β peptide (the most intense band) but also to the oligomeric forms, the strongest interaction being between the oligomeric forms with the GST-R_s recombinant fusion protein (Figure 1B, lane 7). On the other hand, in order to verify that GST protein (GST₀) was not involved in the interaction between A β and the fused proteins GST-R_s, GST-R_d, GST-R_w, and GST-R_t, we examined this possibility by affinity chromatography. As shown in Figure 1B (lane 2), GST₀ had no ability to bind either monomeric or oligomeric A β . Figure 1B (lane 1) represents the reconstitution of synthetic A β (as an internal control) in its different forms visualized by Western blotting. Together, these findings identified that the signal peptide (R_s) of the extracellular domain of integrin β 1 was responsible for binding to A β oligomers *in vitro*.

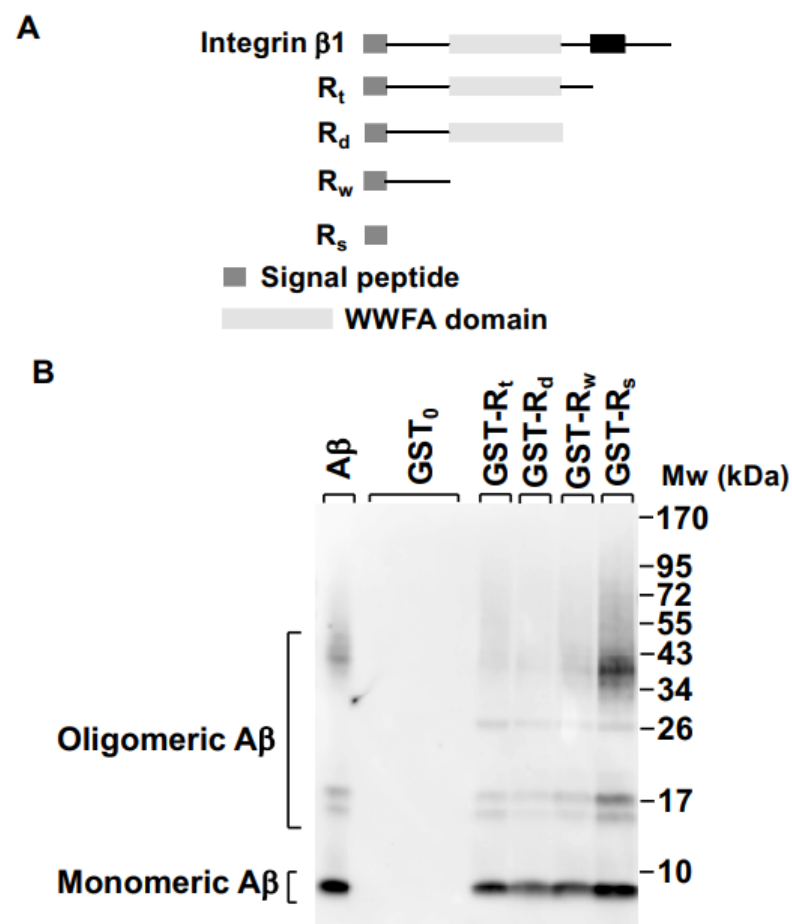


Figure 1. Cont.

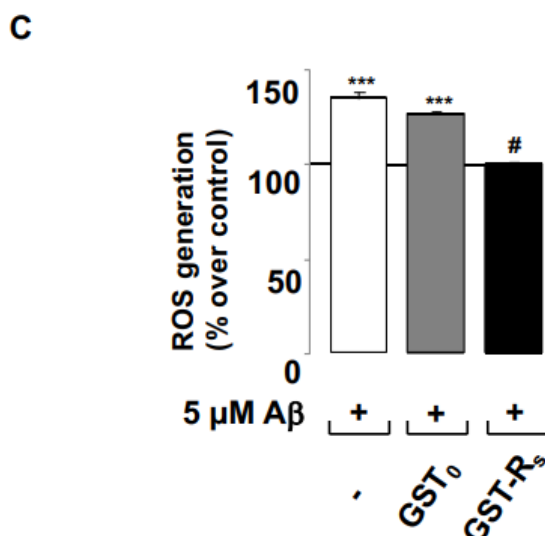


Figure 1. R_s peptide, carrying the signal peptide of integrin β 1, specifically binds to A β peptide and blocks A β -induced ROS production in primary astrocyte cultures. (A) Schematic representation of the structure of integrin β 1 with its different extracellular regions. (B) Interaction of synthetic A β peptide with the indicated GST fusion proteins, GST₀, GST-R_t, GST-R_d, GST-R_w, and GST-R_s. After incubation, glutathione beads were washed and proteins separated by SDS-PAGE under non-reducing conditions and analyzed by Western blot using anti-A β 1–42 antibody (6E10, from Covance). (C) ROS generation was measured by fluorimetry with 10 μM CM-H2DCFDA. Data are expressed as the relative fluorescence normalized to values of untreated or treated cells (100%). *** $p < 0.001$ compared to non-treated cells; # $p < 0.05$ compared to GST₀; unpaired one-way ANOVA.

2.2. R_s Peptide Blocks A β Oligomer-Induced ROS Generation in Cultured Astrocytes

Next, we investigated whether GST-R_s affected ROS generation mediated by A β oligomers in primary astrocyte cultures, as previously shown [38]. For that, we treated primary astrocyte cultures with 5 μM A β oligomers for 60 min alone or together with 5 $\mu\text{g}/\mu\text{L}$ GST₀ (control) or 5 $\mu\text{g}/\mu\text{L}$ GST-R_s, and measured ROS levels by fluorimetry using 10 μM CM-H2DCFDA for 20 min. As expected, A β oligomers induced ROS generation (Figure 1C, empty bar). Regarding GST₀, this peptide did not interfere in A β oligomer-mediated ROS generation (Figure 1C, gray bar). Nevertheless, GST-R_s totally prevented ROS generation mediated by A β oligomers (Figure 1C, solid bar). Taken together, these results show that integrin β 1 signal peptide (R_s) binds *in vitro* to A β oligomers, and that it is able to prevent ROS generation induced by A β oligomers in primary astrocyte cultures.

2.3. A β Oligomers Trigger Gliosis in Mouse Hippocampus *In Vivo*

A β injection in mouse brain causes reactive astrogliosis in the dentate gyrus (DG) [38]. However, it is still unclear whether A β injection in mice brain also drives microgliosis. To investigate that possibility, we performed intrahippocampal injections of vehicle (control) or A β oligomers (A β) and examined astrocyte- and microglia-occupied areas by immunohistochemistry with astrocyte (GFAP and S100 β) and microglia (Iba1) markers in dentate gyrus (DG). As expected, the intrahippocampal administration of A β strongly increased the presence of both the GFAP and S100 β markers compared to control (Figure 2A). In addition, A β also boosted the presence of the Iba1 marker in DG compared to control (Figure 2A). Quantification of the immunohistochemical analysis showed significant increases in the GFAP, S100 β and Iba1 markers in DG values due to A β treatment compared to control (Figure 2B, 1.00 \pm 0.04 vs. 1.21 \pm 0.04 for GFAP, 1.00 \pm 0.04 vs. 1.46 \pm 0.08 for S100 β 1.00 \pm 0.07 vs. 1.31 \pm 0.08 for Iba1). These results confirm that A β induces astrogliosis and show that A β oligomers also lead to microgliosis in adult mouse DG.

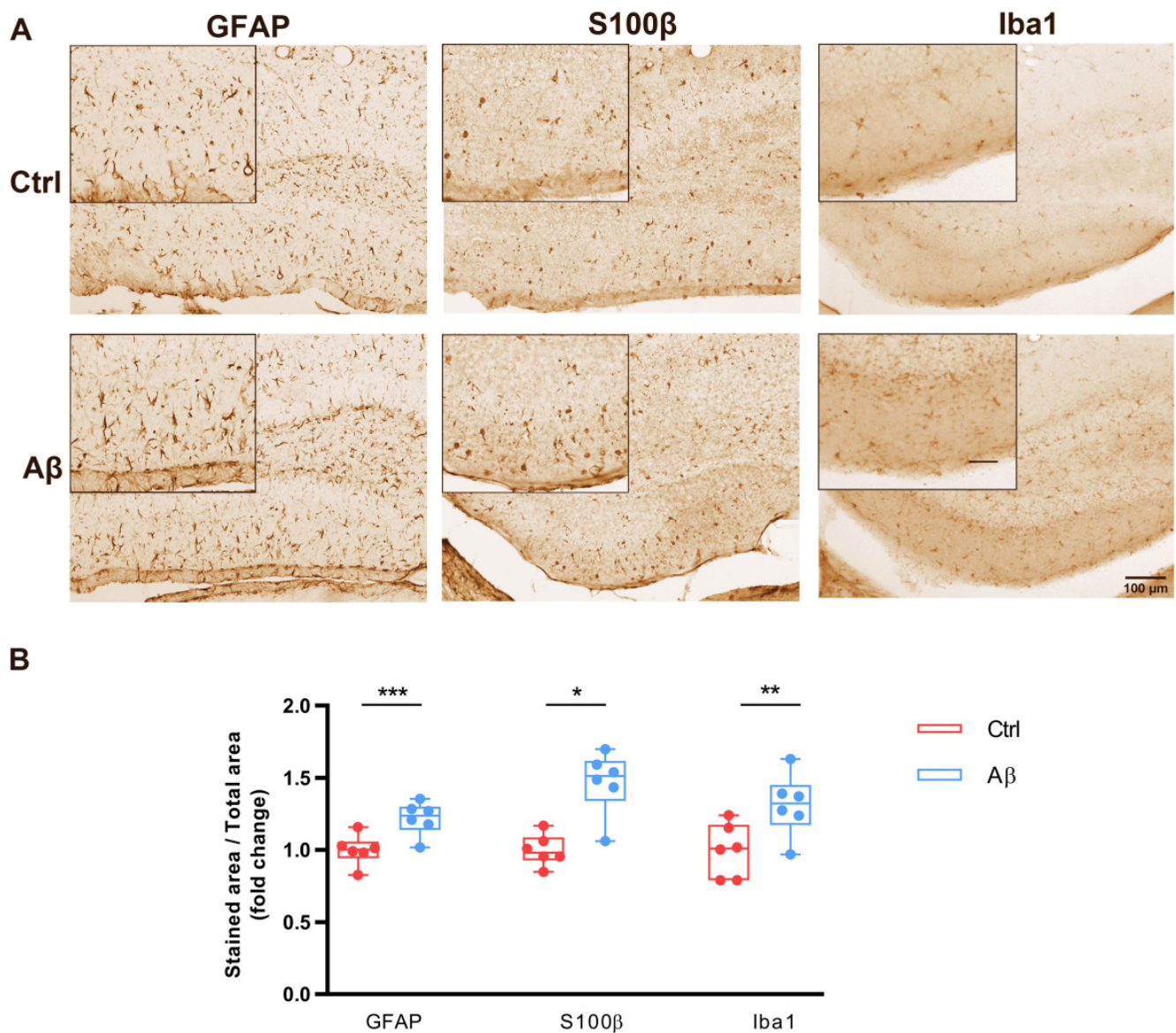


Figure 2. Reactive astrocytes and microglia in the dentate gyrus (DG) of A β -injected mice. **(A)** Coronal sections of mouse brains were immunostained by DAB assay 7 days post-injection with A β or with vehicle (Ctrl). Photomicrographs show GFAP and S100 β immunolabeling in astrocytes and Iba1 immunolabeling in microglia of the dentate gyrus. Scale bar: 100 μ m and Scale bar in zoom is 50 μ m. It is included in caption. Inset: 50 μ m. **(B)** Box plot graphs show quantitative analysis of labelled areas for GFAP, S100 β and Iba1 under A β and control conditions in the DG. Data are presented as the mean \pm S.E.M. Fifteen slices from five animals were analyzed per condition. *** $p < 0.001$, ** $p < 0.01$, * $p < 0.05$ compared with A β -injected mice; unpaired Student's test.

2.4. R_s Peptide Prevents Glia Reactivity in the DG of A β Oligomer-Injected Mice Brain

Before examining the functionality of the GST-R_s fused protein *in vivo*, we evaluated whether GST₀ affected astrocyte and microglia reactivity in A β oligomer-injected brain. For that, we performed intrahippocampal injections of A β and A β with GST₀ (A β + GST₀) and quantified the changes in astrocyte and microglia morphology as described in the previous section. As shown in Figure 3A, the intrahippocampal administration of the combination of A β + GST₀ did not modify the area occupied by both the GFAP and S100 β markers compared to A β alone. However, the area occupied by Iba1 staining appeared increased in the combination A β + GST₀ when it was compared to A β alone (Figure 3A). Quantification of the immunohistochemical analysis showed that GST₀ in the presence

of A β did not produce any significant change in GFAP and S100 β staining (Figure 3B; 0.94 ± 0.09 vs. 0.64 ± 0.03 for GFAP, 0.93 ± 0.08 vs. 0.67 ± 0.06 for S100 β , whereas it caused microgliosis as compared to A β alone (1.00 ± 0.04 vs. 0.77 ± 0.03 for Iba1). These results suggest that the GST $_0$ protein did not reduce A β -dependent astrogliosis and/or microgliosis.

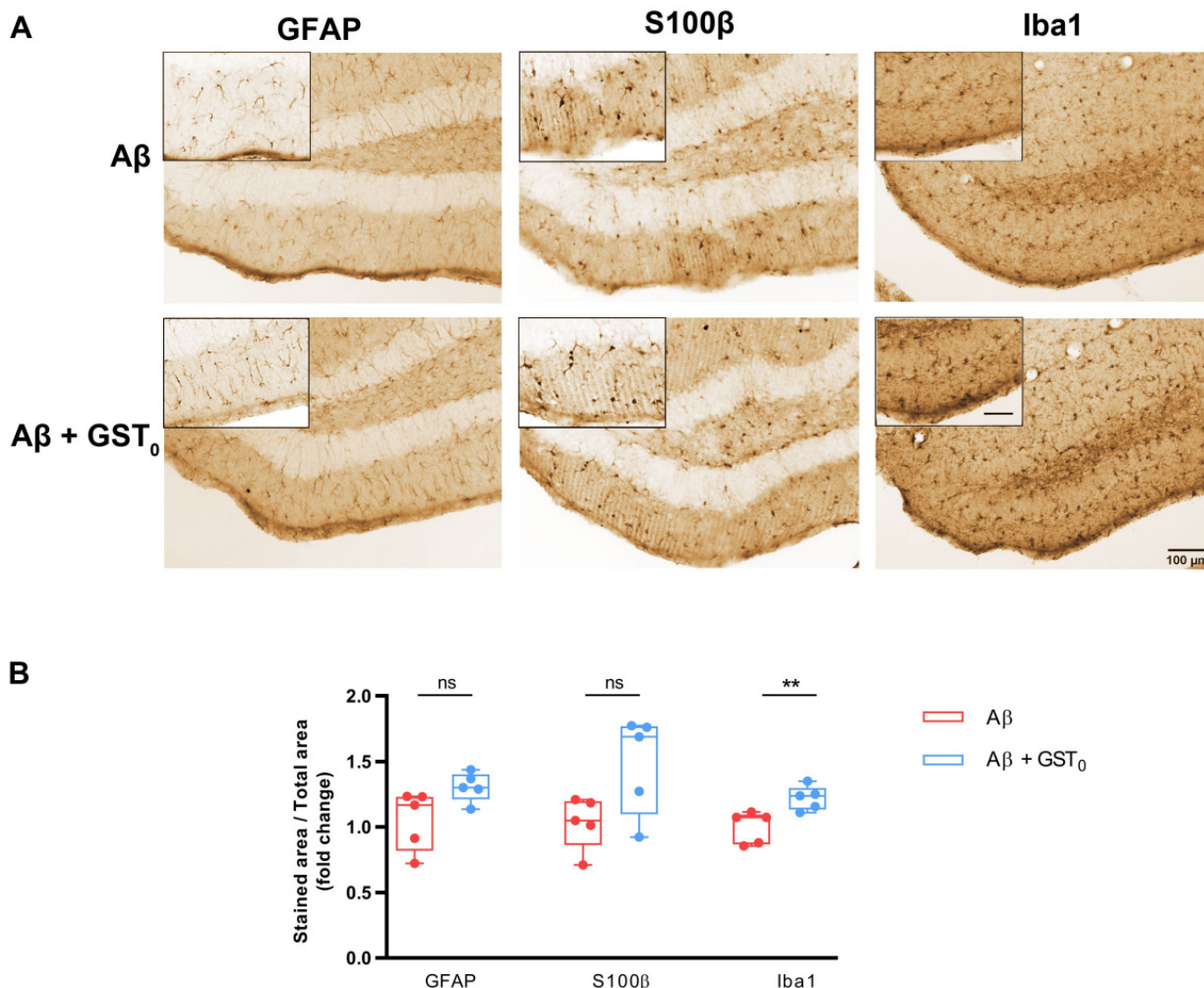


Figure 3. GST $_0$ polypeptide is ineffective in preventing gliosis in the DG of A β -injected mice. (A) Coronal sections of mouse brains were immunostained by DAB assay 7 days post-injection with A β and A β + GST $_0$. Photomicrographs show GFAP and S100 β immunolabeling in astrocytes and Iba1 immunolabeling in microglia of the dentate gyrus. Scale bar: 100 μ m and Scale bar in zoom is 50 μ m. It is included in caption: 50 μ m. (B) Box plot graphs show quantitative analysis of labelled areas for GFAP, S100 β and Iba1 under A β and A β + GST $_0$ in the DG. Data are presented as the mean \pm S.E.M. Fifteen slices from five animals were analyzed per condition. ns: non-significant; ** $p < 0.01$ compared with A β -injected mice; unpaired Student's test.

Based on that, we examined the ability of recombinant GST-R $_s$ peptide to prevent A β -mediated astrogliosis in brain. For that, we performed intrahippocampal injections of A β , and A β with GST-R $_s$ peptide (A β + GST-R $_s$) and the glial changes were analyzed and quantified. As shown in Figure 4A, the intrahippocampal administration of the combination of A β + GST-R $_s$ strongly reduced the presence of three—GFAP, S100 β and Iba1—markers compared to A β .

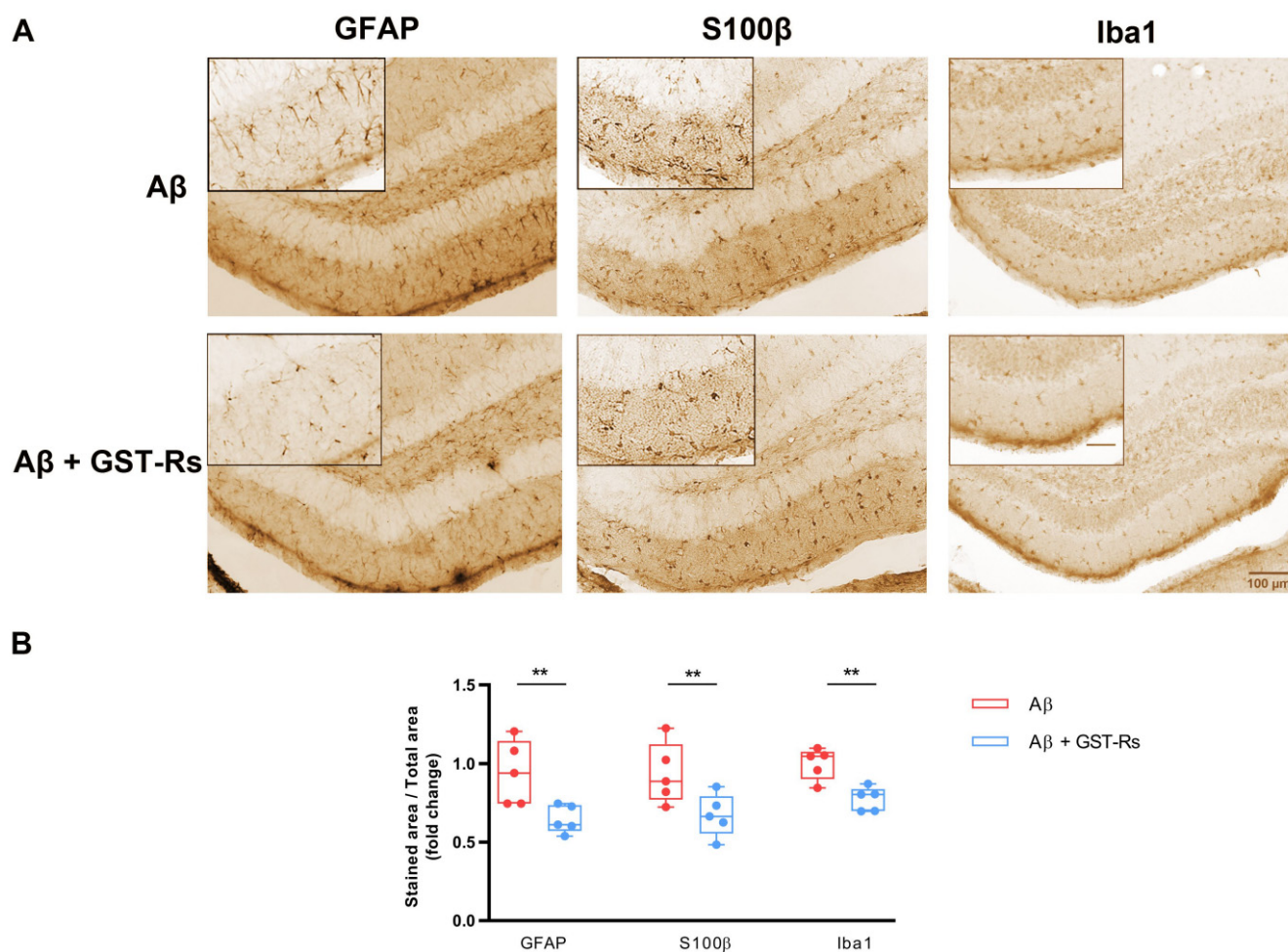


Figure 4. GST-R_s polypeptide prevents gliosis in the DG of Aβ-injected mice. (A) Coronal sections of mouse brains were immunostained by DAB assay 7 days post-injection with Aβ or Aβ + GST-R_s. Photomicrographs show GFAP and S100β immunolabeling in astrocytes and Iba1 immunolabeling in microglia of the dentate gyrus. Scale bar: 100 μm and Scale bar in zoom is 50 μm. It is included in caption. 50 μm (B) Box plot graphs show quantitative analysis of labelled areas for GFAP, S100β and Iba1 under Aβ and Aβ + GST-R_s in the DG. Data are presented as the mean ± S.E.M. Fifteen slices from five animals were analyzed per condition. ** *p* < 0.01 compared with Aβ-injected mice; unpaired Student's test.

Quantification of the immunohistochemical analysis showed a significant decrease in GFAP, S100β and Iba 1 (Figure 4B) in the presence of Aβ + GST-R_s compared to Aβ (1.05 ± 0.10 vs. 1.30 ± 0.05 for GFAP, 1.03 ± 0.08 vs. 1.484 ± 0.167 for S100β 1.00 ± 0.05 vs. 1.22 ± 0.04 for Iba1). These results point out that integrin β1 signal peptide R_s blocks Aβ-induced not only astrogliosis but also in microgliosis in adult mouse DG.

2.5. R_s Peptide Reduces Endoplasmic Reticulum Stress in Astrocytes in DG of Aβ Oligomer-Injected Mice Brain

Acute injection of Aβ oligomers in mouse brain induces GRP78 chaperone protein over-expression particularly in astrocytes [39], being used as an endoplasmic reticulum stress marker. Therefore, we investigated whether recombinant R_s fused protein to GST (GST-R_s) could also prevent endoplasmic reticulum stress in astrocytes after intrahippocampal Aβ injection. Accordingly, we carried out a double immunostaining assay for S100β and GRP78 of brain tissues previously injected with Aβ, Aβ + GST-R_s and Aβ + GST₀. Intrahippocampal administration of the combination of recombinant GST-R_s peptide and Aβ oligomers strongly reduced GRP78 expression in S100β-positive astrocytes compared

to A β oligomers alone (Figure 5A,B). Furthermore, the combination of GST₀ and A β oligomers did not alter the effect induced by A β alone (Figure 5B). Quantification of immunofluorescence staining showed a significant decrease in GRP78 in S100 β values in DG from brains injected with GST-R_s fusion protein compared to control (A β -injected mice) (26.95 ± 1.01 vs. 30.64 ± 1.24) (Figure 5A). In contrast, GST₀ protein did not produce any effect in A β -induced endoplasmic reticulum stress in S100 β (Figure 5B) values compared to A β alone (21.42 ± 2.48 vs. 22.07 ± 1.36). These findings suggest that R_s also prevents endoplasmic reticulum stress induced by A β oligomers.

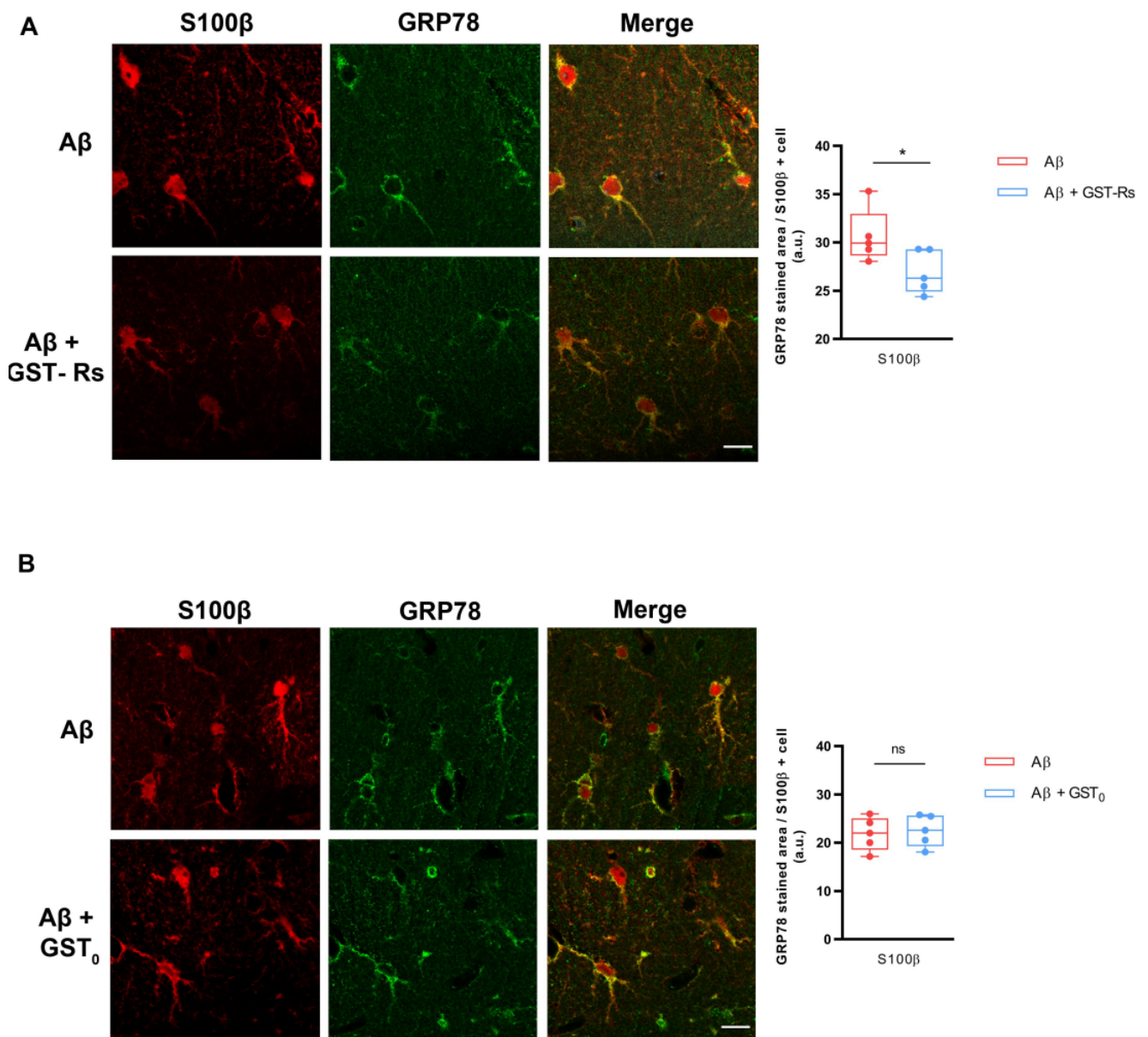


Figure 5. GST-R_s polypeptide reduces GRP78 expression in S100 β -positive astrocytes of A β -injected mouse brains. Photomicrographs of double immunofluorescence staining for S100 β (red) and GRP78 (green) on DG of animals injected with different: A β and A β + GST-R_s (A) or A β and A β + GST₀ (B). Quantitative analysis of fluorescence intensity was performed for GRP78 levels in S100 β -positive astrocytes in dentate gyrus after A β and A β + GST-R_s (A) or A β and A β + GST₀ (B). Scale bar in zoom area: 20 μ m. Data are presented as the mean \pm SEM. Fifteen slices from five animals were analyzed per condition. ns: non-significant; * $p < 0.05$ compared with A β -injected mouse; unpaired Student's test.

3. Discussion

Our study identifies the integrin $\beta 1$ minimal region that binds to $A\beta$ oligomers. This region spans from aa 1 to aa 20 and corresponds to integrin $\beta 1$ signal peptide (R_s peptide). From a functional point of view, this peptide is a very useful tool to block $A\beta$ oligomer-induced ROS generation in primary astrocyte cultures and also in vivo when R_s peptide in combination with $A\beta$ oligomers is directly injected into the mice hippocampus. In this scenario, astroglial stress, astrogliosis and even microgliosis induced by $A\beta$ oligomers are efficiently prevented.

Several investigations postulate that there are many potential receptors localized at neuronal synapses with both high affinity for $A\beta$ peptide and the ability to intracellularly transduce the toxic instructions emanating from $A\beta$ oligomers [40]. These include NMDA receptors that are directly activated by $A\beta$ oligomers, altering its physiological function [41], although those that seem to be acquiring increasing relevance are integrins. In fact, the interaction between integrins and $A\beta$ oligomers promotes neurotoxicity, inhibition of LTP and an increase in spine density [26,42]. In this regard, synthetic $A\beta$ monomer binds through its amino acid sequence RHDS to the $\alpha 2\beta 3$ integrin, being directly related to cerebral amyloid angiopathy, which contributes to dementia and AD [43].

Integrins control important cellular responses including proliferation, survival and cell migration [44]. All of them require the active participation of transducing molecules such as tyrosine kinases FAK, ILK and Src or small GTPases of the Rho family [44]. In addition, PKCs may also be involved in integrin-mediated signaling [45]. We have previously observed that $A\beta$ oligomer-induced PKC phosphorylation is mediated by integrin $\beta 1$ in astrocytes and in neurons [38]. Further, $A\beta$ oligomers lead to NR2B subunit upregulation on neuronal membranes through the PKC signaling pathway [46]. Under these circumstances, integrin $\beta 1$ transduces the message that $A\beta$ oligomers brings, generating a cellular response which manifests itself in a higher permeability for calcium ions to alter cellular homeostasis [46]. Hence, depending on the stimulus or ligands, the same receptor along with its intracellular signaling molecules can switch on/off different pathways that lead to antagonistic cellular responses.

Currently, in addition to pharmacotherapy, gene therapeutic approaches for AD have entered phase I/II clinical trials [47]. The results of this preliminary study obtained with recombinant R_s allow us to postulate a new pharmacological therapeutic alternative in AD. This recombinant peptide neutralizes $A\beta$ oligomer activity from outside the cell (Figure 6 panel B compared to panel A). In addition, R_s recombinant peptide is a useful tool that will aid understanding the molecular mechanisms of the deleterious actions initiated by $A\beta$ oligomers both in vitro and in vivo.

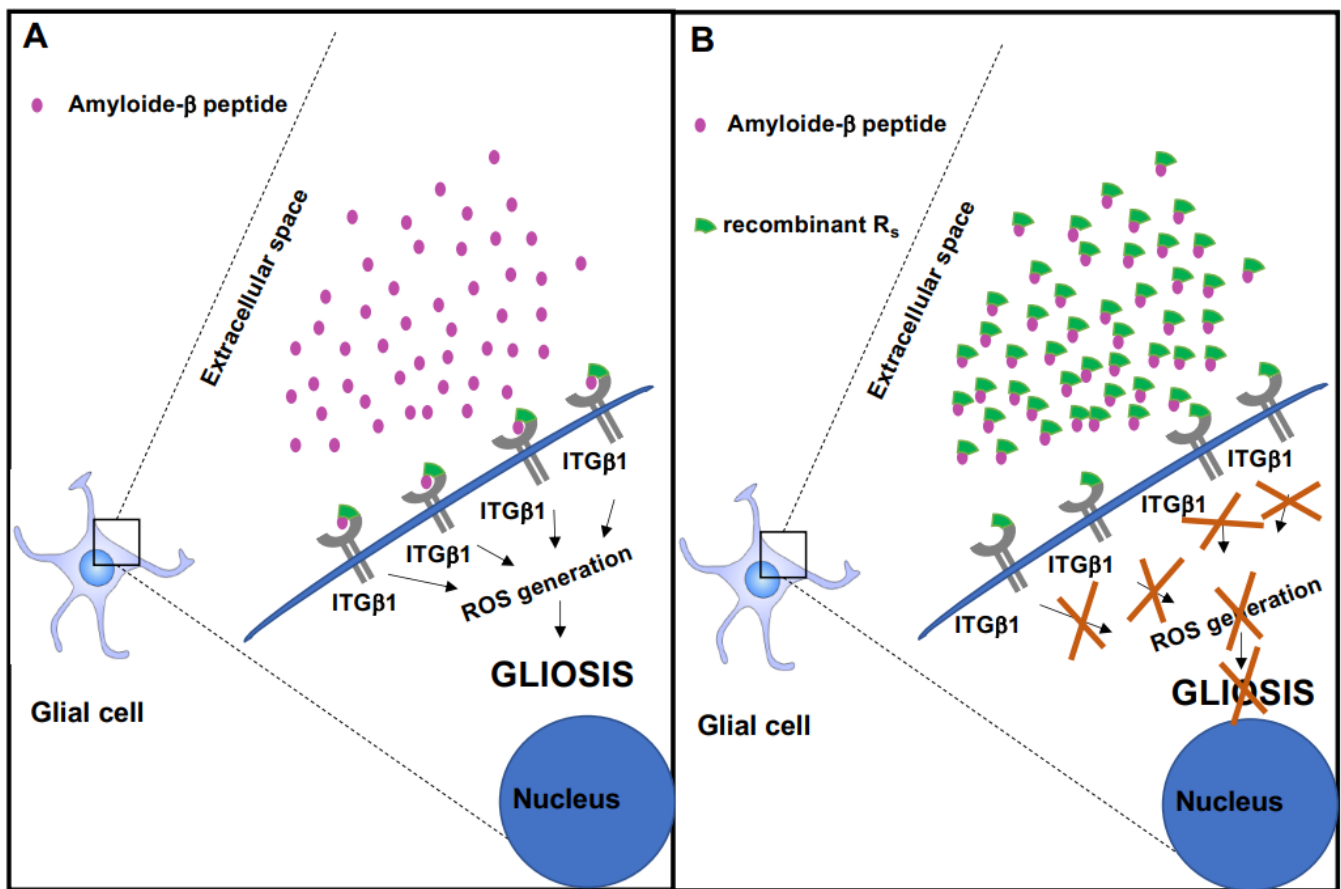


Figure 6. Functional model of recombinant R_s peptide to prevent the toxic effect from amyloide β peptide. (A) Amyloide β peptide from the extracellular space binds to integrin β 1 and triggers the activation of intracellular signaling pathways that lead to the generation of reactive oxygen species and gliosis. (B) Recombinant R_s peptide and amyloide β peptide interact with each other; and in these circumstances, amyloide β peptide cannot bind to the R_s region of integrin β 1 and does not activate the signaling pathways that lead to ROS generation and gliosis.

4. Conclusions

We and others have described a key molecular relationship between integrin β 1 and A β peptides required to modulate neuronal and glial biology [27,38,42,46]. The findings point out the molecular mechanism by which recombinant R_s peptide works in order to block A β oligomer intracellular signaling both in vitro and in vivo. The presence of this recombinant peptide in the extracellular medium interferes with binding between A β oligomers and its receptor, integrin β 1, since the R_s peptide associates with A β oligomers, thus preventing it from binding to the endogenous integrin β 1, and consequently avoiding the transmission of its toxic message. In fact, R_s peptide blocks ROS generation induced by A β oligomers and at the same time significantly reduces astroglial stress, astroglial gliosis and microglial gliosis. It is important to highlight that R_s peptide in turn protects the functional receptorial properties of integrin β 1, allowing integrin β 1 in the cell membrane to be accessible to physiological activators (Figure 6). Future studies will allow us to investigate the efficacy of this peptide in preventing A β oligomers binding to other receptors.

5. Experimental Procedures

Animals. All experimental procedures (M20-2017-092) followed the European Directive 2010/63/EU and were approved by the ethics committee of the University of the Basque Country (UPV/EHU). Animals were housed in standard conditions under 12 h light/dark cycle and with ad libitum access to food water. All possible effort was made to

minimize animal suffering and the number of animals used. Experiments were performed in C57BL6/J mice.

Preparation of A β _{1–42} Oligomers. A β _{1–42} oligomers were prepared as reported previously [48]. Briefly, A β _{1–42} was initially dissolved to 1 mM in hexafluoroisopropanol (Merck Life Science S.L.U., Madrid, Spain) and distributed aliquoted in sterile microcentrifuge tubes. Hexafluoroisopropanol was totally removed under vacuum in a speed vac system and the peptide film was stored at -80°C . For the aggregation protocol, the peptide was first resuspended in anhydrous DMSO (Merck Life Science S.L.U., Madrid, Spain) to a concentration of 5 mM, to finally bring the peptide to a final concentration of 100 μM in Hams F-12 (Merck Life Science S.L.U., Madrid, Spain) and to incubate it at 4°C for 24 h. The preparation was then centrifuged at $14,000\times g$ for 10 min, at 4°C , to remove insoluble aggregates and the supernatants containing soluble A β _{1–42} were transferred to clean tubes and stored at 4°C .

Plasmid Construct. The ITG β 1 fragments comprising amino acids 1–20 (R_s), 1–140 (R_w), 1–371 (R_d) and 1–728 (R_t) were generated by PCR amplification using pCMV6-XL5-ITGB1 (from Origene Technologies Inc. Rockville, MD, USA) as template (forward oligonucleotide, 5'-CGG AAT TCA TGA ATT TAC AAC C-3' and reverse oligonucleotides, 5'-CGG AAT TCA GCA AAC ACA CAG C-3', 5'-CGG AAT TCG TCT TCA GCT CTC T-3', 5'-CGG AAT TCA AGG GAA TTG TAT G-3', 5'-CGG AAT TCG TCT GGA CCA GTG G-3', each harboring EcoRI restriction sites (underlined). The EcoRI ITG β 1 extracellular fragments were subcloned into pGEX-4T3 (Merck Life Science S.L.U., Madrid, Spain) to generate the GST-R_s, GST-R_w, GST-R_d and GST-R_t fusion proteins. All GST-fused peptides were purified by affinity chromatography onto glutathione beads following standard procedures [49].

Binding Assay. In vitro binding assays with recombinant fusion proteins were performed as previously described [50]. Briefly, glutathione beads coated with recombinant fusion proteins (500 ng GST₀, GST-R_t, GST-R_w, GST-R_d or GST-R_s) were incubated with 100 pM A β oligomers in binding buffer (50 mM Tris-HCl pH7.5, 5 mM MgCl₂, 20 mM KCl, 500 $\mu\text{g}/\text{mL}$ BSA) for 1 h at RT. Immobilized GST beads were washed twice with binding buffer and five times with 50 mM Tris-HCl pH 7.5, 150 mM NaCl. Proteins were eluted adding sample buffer under non-reducing conditions and separated by SDS-PAGE followed by Western blot. Immunoreactive bands were visualized with anti-6E10 antibody and ECL.

Astrocyte Culture. Primary cultures of cerebral cortical astrocytes were prepared from P₀–P₂ Sprague Dawley rats as previously described [51]. Cortical lobes were extracted and enzymatically digested with 400 μL of 2.5% trypsin and 40 μL of 0.5% deoxyribonuclease in Hank's Balanced Salt Solution (HBSS, Merck Life Science S.L.U., Madrid, Spain) for 15 min at 37°C . The enzymatic reaction was stopped by adding IMDM medium supplemented with 10% FBS (Thermo Fisher Scientific, Madrid, Spain) and centrifuged at $300\times g$ for 6 min. The cell pellet was resuspended in 1 mL of the same solution and mechanical dissociation was performed by using 21- and 23G-gauge cutting needles. The resulting cell suspension was centrifuged at $300\times g$ for 6 min and plated onto 75 cm² flasks coated with 30 $\mu\text{g}/\text{mL}$ Poly-D-Lysine. After 8 DIV, cells were plated onto PDL-coated plates and maintained for 2 days. The culture medium was replaced with IMDM with 1% FBS 24 h before A β treatment.

Measurement of Intracellular Reactive Oxygen Species. For the quantification of generated ROS in treated cells, fluorescent dye 5-(and 6)-chloromethyl-2',7-dichlorodihydrofluorescein diacetate acetyl ester (CM-H2DCFDA) was used. Astrocytes (1×10^4) were exposed to 5 μM A β oligomers [29,30] alone or together with 5 $\mu\text{g}/\mu\text{L}$ GST₀ or 5 $\mu\text{g}/\mu\text{L}$ GST-R_s and loaded with 10 μM CM-H2DCFDA for 30 min immediately after the treatment. After three washes with PBS, ROS levels were measured with excitation and emission wavelengths of 485 and 520 nm, respectively.

Intrahippocampal Injection in Adult Mice. Adult male mice (3–4 months) were randomized, anesthetized with ketamine hydrochloride ($80\text{ mg}\times\text{kg}^{-1}$) and xylazine ($10\text{ mg}\times\text{kg}^{-1}$), and injected stereotaxically into the hippocampus at the following coordinates: 2.2 mm from Bregma, 1.5 mm lateral to the sagittal suture, and 2 mm from the

pial surface. Mice were divided into four groups ($n = 5\text{--}6$ per group) and injected with 3 μL of either vehicle (17% DMSO + 83% Ham's F12; control), A β oligomers (10 μM ; A β), A β plus GST $_0$ (10 μM and 0.45 $\mu\text{g}/\mu\text{L}$, respectively; A β + GST $_0$), or A β plus R $_s$ peptide (10 μM and 0.45 $\mu\text{g}/\mu\text{L}$, respectively; A β + R $_s$). After 7 days, mice were anesthetized with ketamine hydrochloride (80 $\text{mg} \times \text{kg}^{-1}$) and xylazine (10 $\text{mg} \times \text{kg}^{-1}$) and perfused with 30 mL of phosphate buffer followed by 30 mL of 4% PFA (paraformaldehyde) in 0.4 M PBS (pH 7.5). The brains were extracted and post-fixed with the same fixative solution for 4 h at RT, placed in 30% sucrose in 0.1 M PBS pH 7.5 at 4 °C, and then kept in cryoprotectant solution (30% ethylene glycol, 30% glycerol and 0.1 M PBS in dH $_2$ O) at -20 °C.

Brain Slice Preparation and Immunostaining. Brain tissue was cut using a Leica VT 1200S vibrating blade microtome (Leica microsystems). Coronal 40 μm thick sections were washed in PBS and incubated with 0.1 M PBS containing 3% H $_2$ O $_2$ for 10 min at RT. Then, slices were rinsed three times with PBS and blocked in blocking solution (PBS pH 7.5, 4% HS, 0.1% Triton X-100) for 30 min at RT. Next, slices were incubated with the corresponding specific primary antibodies (rabbit anti-GFAP (1:1000 from Merck Life Science S.L.U., Madrid, Spain), rabbit anti-S100 β (1:500 from Dako, Glostrup, Denmark) or rabbit anti-Iba1 (1:250 from Fujifilm Wako Chemicals, Richmond, VA, USA), in the same blocking solution, overnight at 4 °C with gentle shaking. Next, slices were washed three times with PBS and incubated with secondary antibodies (1:500 from Vector Laboratories Burlingame, CA, USA) in the blocking solution for 1 h at RT. Slices were incubated with the ABC complex following the manufacturer's instructions (Vector Laboratories, Burlingame, CA, USA) for 1 h at RT and washed three times with PBS. Slices were treated with DAB (Vector Laboratories Burlingame, CA, USA) according to the manufacturer's instructions and washed three times with PBS. Finally, slices were mounted on glass slides with DPX.

For immunofluorescence of brain slices, slices were kept in PBS at 4 °C and permeabilized and blocked with 0.1 M PBS pH 7.5, 10% NGS, and 0.1% Triton X-100 for 1 h at RT. Slices were incubated with primary antibodies (rabbit anti-S100 β (1:500 from Dako, Glostrup, Denmark) and mouse anti-GRP78 (1:500 from Elabscience, Houston, TX, USA)) overnight at 4 °C with gentle shaking. Slices were then washed three times with 0.1 M PBS pH 7.5, 0.1% Triton X-100 (washing buffer) and incubated with blocking solution containing fluorochrome-conjugated secondary antibodies for 1 h at RT. After that, slices were washed three times with washing buffer, incubated with 4 $\mu\text{g}/\text{mL}$ DAPI, washed twice again with washing buffer and mounted on glass slides with Fluoromount-G mounting medium (SouthernBiotech, Birmingham, AL, USA).

Image acquisition and analysis. Brightfield images were acquired with the Panoramic MIDI II automated digital slide scanner (3DHistech Ltd., Budapest, Hungary). To analyze reactive gliosis, the area occupy by DAB divided by total area was measured.

Fluorescence immunostaining was observed with a Leica TCS SP8 microscope using a 63 \times oil-immersion objective to generate z-stack projections. For fluorescence intensity analysis, images were taken with the same settings for all experiment and the mean value along the stack profile was quantified with LAS AF Lite software, version 4.0, Leica Microsystems CMS GmbH, Shinjuku, Tokyo, Japan (Leica).

Statistical analysis. All data were expressed as the mean \pm S.E.M. Statistical analyses were performed using absolute values. GraphPad Prism software (<https://www.graphpad.com/scientific-software/prism/>, accessed on 1 April 2022) was used applying one-way analysis of variance with post hoc Fisher's least significant difference (LSD) test for multiple comparisons and two-tailed, unpaired Student's *t* test for comparison of the two groups and control conditions.

Author Contributions: Conceptualization, E.A. and J.L.Z.; data curation, C.O.-S., F.L., J.Z.-I., U.B., T.Q.-L., A.W., E.C.-Z., C.M., E.A. and J.L.Z.; methodology, C.O.-S., F.L., J.Z.-I., U.B., T.Q.-L., A.W. and E.C.-Z.; in vivo injections, C.M., E.A. and C.O.-S.; validation, E.C.-Z., C.M., E.A. and J.L.Z.; formal analysis, C.O.-S., F.L., E.C.-Z., C.M., E.A. and J.L.Z.; resources, E.C.-Z., C.M., E.A., J.L.Z. and F.L.; writing—original draft preparation, C.O.-S., F.L., E.A. and J.L.Z.; writing—review and editing, E.A. and J.L.Z.; visualization, E.A. and J.L.Z.; supervision, E.A. and J.L.Z.; project administration, E.A. and

J.L.Z.; funding acquisition, E.C.-Z., C.M., E.A. and J.L.Z. All authors have read and agreed to the published version of the manuscript.

Funding: E.A. was supported by MICINN (PID2019-108465RB-I00) and Basque Government (PIBA_2020_1_0012). C.M. was supported by MICINN (PID2019-109724RB-I00), Basque Government (IT1203-19) and CIBERNED (CB06/0005/0076). E.C.-Z. was supported by Basque Government (ELKARTEK KK-2020/00034; PIBA_2016_1_0009). J.L.Z. was supported by the Instituto de Salud Carlos III (PI18/00207), Basque Government (PIBA_2020_1_0048) and University of Basque Country Grant (US19/04).

Institutional Review Board Statement: Not applicable.

Informed Consent Statement: All authors qualify for authorship, approved the final version of the manuscript and agree to be accountable for all aspects of the work in ensuring that questions related to the accuracy or integrity of any part of the work are appropriately investigated and resolved.

Data Availability Statement: The datasets generated and/or analyzed during the current study are available from the corresponding authors on reasonable request.

Conflicts of Interest: The authors have no relevant financial or non-financial interests to disclose. The authors declare that they have no conflict of interest with the contents of this article.

Abbreviations

A β —amyloid β protein fragment 1–42; AD—Alzheimer’s disease; AKT—protein kinase B; CM-H2DCFDA—5-(and-6)-chloromethyl-2',7'-dichlorodihydrofluorescein diacetate, acetyl ester; DAB—3, 3'-diaminobenzidine; CSF—cerebrospinal fluid; DAPI—4',6-diamidino-2-phenylindole; DMSO—dimethyl sulfoxide; DPX—distyrene, a plasticizer and xylene; ECM—extracellular matrix; ERK—extracellular signal-regulated kinase; FAK—focal adhesion kinase; GFAP—glial fibrillary acid protein; GST—glutathione S-transferase; ILK—integrin-linked kinase; ITG β 1—integrin β 1; JNK—c-Jun N-terminal kinase; NFT—neurofibrillary tangles; ROS—reactive oxygen species; ICAM-1—intracellular adhesion molecule-1; NMDA—N-methyl-D-aspartate.

References

1. Barker, W.W.; Luis, C.A.; Kashuba, A.; Luis, M.; Harwood, D.G.; Loewenstein, D.; Waters, C.; Jimison, P.; Shepherd, E.; Sevush, S.; et al. Relative frequencies of Alzheimer disease, Lewy body, vascular and frontotemporal dementia, and hippocampal sclerosis in the state of Florida brain Bank. *Alzheimer Dis. Assoc. Disord.* **2002**, *16*, 203–212. [[CrossRef](#)] [[PubMed](#)]
2. Alzheimer, A.; Stelzmann, R.A.; Schnitzlein, H.N.; Murtagh, F.R. An English translation of Alzheimer’s 1907 paper, “Über eine eigenartige Erkrankung der Hirnrinde”. *Clin. Anat.* **1995**, *8*, 429–431. [[CrossRef](#)] [[PubMed](#)]
3. Kumar, A.; Singh, A.; Ekavali. A review on Alzheimer’s disease pathophysiology and its management: An update. *Pharmacol. Rep.* **2015**, *67*, 195–203. [[CrossRef](#)] [[PubMed](#)]
4. Goedert, M. Oskar Fischer and the study of dementia. *Brain* **2009**, *132*, 1102–1111. [[CrossRef](#)]
5. Thal, D.R.; Capetillo-Zarate, E.; Del Tredici, K.; Braak, H. The development of amyloid beta protein deposits in the aged brain. *Sci. Aging Knowl. Environ.* **2006**, *2006*, re1. [[CrossRef](#)]
6. DeTure, M.A.; Dickson, D.W. The neuropathological diagnosis of Alzheimer’s disease. *Mol. Neurodegener.* **2019**, *14*, 32. [[CrossRef](#)]
7. Braak, H.; Braak, E. Frequency of stages of Alzheimer-related lesions in different age categories. *Neurobiol. Aging* **1997**, *18*, 351–357. [[CrossRef](#)]
8. Glenner, G.G.; Wong, C.W. Alzheimer’s disease and Down’s syndrome: Sharing of a unique cerebrovascular amyloid fibril protein. *Biochem. Biophys. Res. Commun.* **1984**, *16*, 1131–1135. [[CrossRef](#)]
9. Hardy, J.A.; Higgins, G.A. Alzheimer’s disease: The amyloid cascade hypothesis. *Science* **1992**, *256*, 184–185. [[CrossRef](#)]
10. Selkoe, D.J. The molecular pathology of Alzheimer’s disease. *Neuron* **1991**, *6*, 487–498. [[CrossRef](#)]
11. Glenner, G.G.; Wong, C.W. Alzheimer’s disease: Initial report of the purification and characterization of a novel cerebrovascular amyloid protein. *Biochem. Biophys. Res. Commun.* **1984**, *120*, 885–890. [[CrossRef](#)]
12. Hardy, J.; Allsop, D. Amyloid deposition as the central event in the aetiology of Alzheimer’s disease. *Trends Pharmacol. Sci.* **1991**, *12*, 383–388. [[CrossRef](#)]
13. Hardy, J.; Selkoe, D.J. The Amyloid Hypothesis of Alzheimer’s Disease: Progress and Problems on the Road to Therapeutics. *Science* **2002**, *297*, 353–356. [[CrossRef](#)] [[PubMed](#)]

14. Grangeon, L.; Cassinari, K.; Rousseau, S.; Croisile, B.; Formaglio, M.; Moreaud, O.; Boutonnat, J.; Le Meur, N.; Miné, M.; Coste, T.; et al. Early-Onset Cerebral Amyloid Angiopathy and Alzheimer Disease Related to an APP Locus Triplication. *Neurol. Genet.* **2021**, *7*, e609. [[CrossRef](#)]
15. Hampel, H.; Vergallo, A.; Caraci, F.; Cuello, A.C.; Lemercier, P.; Vellas, B.; Virecoulon Giudici, K.; Baldacci, F.; Hanisch, B.; Haberkamp, M.; et al. Future avenues for Alzheimer's disease detection and therapy: Liquid biopsy, intracellular signaling modulation, systems pharmacology drug discovery. *Neuropharmacology* **2021**, *185*, 108081. [[CrossRef](#)]
16. Oddo, S.; Caccamo, A.; Shepherd, J.D.; Murphy, M.P.; Golde, T.E.; Kaye, R.; Metherate, R.; Mattson, M.P.; Akbari, Y.; LaFerla, F.M. 3xTg-AD model of Alzheimer's disease with plaques and tangles intracellular A β and synaptic dysfunction. *Neuron* **2003**, *39*, 409–421. [[CrossRef](#)]
17. Tomiyama, T.; Matsuyama, S.; Iso, H.; Umeda, T.; Takuma, H.; Ohnishi, K.; Ishibashi, K.; Teraoka, R.; Sakama, N.; Yamashita, T.; et al. A Mouse Model of Amyloid Oligomers: Their Contribution to Synaptic Alteration, Abnormal Tau Phosphorylation, Glial Activation, and Neuronal Loss In Vivo. *J. Neurosci.* **2010**, *30*, 4845–4856. [[CrossRef](#)]
18. Bao, F.; Wicklund, L.; Lacor, P.N.; Klein, W.L.; Nordberg, A.; Marutle, A. Different β -amyloid oligomer assemblies in Alzheimer brains correlate with age of disease onset and impaired cholinergic activity. *Neurobiol. Aging* **2012**, *33*, 825.e1–825.e13. [[CrossRef](#)]
19. Santos, A.N.; Ewers, M.; Minthon, L.; Simm, A.; Silber, R.E.; Blennow, K.; Prvulovic, D.; Hansson, O.; Hampel, H. Amyloid- β oligomers in cerebrospinal fluid are associated with cognitive decline in patients with Alzheimer's disease. *J. Alzheimer Dis.* **2012**, *29*, 171–176. [[CrossRef](#)]
20. Alberdi, E.; Sánchez-Gómez, M.V.; Cavaliere, F.; Peérez-Samartín, A.; Zugaza, J.L.; Trullas, R.; Domercq, M.; Matute, C. Amyloid β oligomers induce Ca²⁺ dysregulation and neuronal death through activation of ionotropic glutamate receptors. *Cell Calcium* **2010**, *47*, 264–272. [[CrossRef](#)]
21. Lambert, M.P.; Barlow, A.K.; Chromy, B.A.; Edwards, C.; Freed, R.; Liosatos, M.; Morgan, T.E.; Rozovsky, I.; Trommer, B.; Viola, K.L.; et al. Diffusible, nonfibrillar ligands derived from Abeta1-42 are potent central nervous system neurotoxins. *Proc. Natl. Acad. Sci. USA* **1998**, *95*, 6448–6453. [[CrossRef](#)] [[PubMed](#)]
22. Wang, Q.; Walsh, D.M.; Rowan, M.J.; Selkoe, D.J.; Anwyl, R. Block of Long-Term Potentiation by Naturally Secreted and Synthetic Amyloid—Peptide in Hippocampal Slices Is Mediated via Activation of the Kinases c-Jun N-Terminal Kinase, Cyclin-Dependent Kinase 5, and p38 Mitogen-Activated Protein Kinase as well as metabotropic glutamate receptor type 5. *J. Neurosci.* **2004**, *24*, 3370–3378. [[CrossRef](#)] [[PubMed](#)]
23. Demuro, A.; Mina, E.; Kaye, R.; Milton, S.C.; Parker, I.; Glabe, C.G. Calcium Dysregulation and Membrane Disruption as a Ubiquitous Neurotoxic Mechanism of Soluble Amyloid Oligomers. *J. Biol. Chem.* **2005**, *280*, 17294–17300. [[CrossRef](#)] [[PubMed](#)]
24. Viola, K.L.; Klein, W.L. Amyloid β oligomers in Alzheimer's disease pathogenesis, treatment, and diagnosis. *Acta Neuropathol.* **2015**, *129*, 183–206. [[CrossRef](#)]
25. Verdier, Y.; Zarándi, M.; Penke, B. Amyloid β -peptide interactions with neuronal and glial cell plasma membrane: Binding sites and implications for Alzheimer's disease. *J. Pept. Sci.* **2004**, *10*, 229–248. [[CrossRef](#)]
26. Wang, Q.; Klyubin, I.; Wright, S.; Griswold-Prenner, I.; Rowan, M.J.; Anwyl, R. α v Integrins mediate beta-Amyloid induced inhibition of long-term potentiation. *Neurobiol. Aging* **2008**, *29*, 1485–1493. [[CrossRef](#)] [[PubMed](#)]
27. Wang, N.; Butler, J.P.; Ingber, D.E. Mechanotransduction across the cell surface and through the cytoskeleton. *Science* **1993**, *21*, 1124–1127. [[CrossRef](#)]
28. Davis, T.L.; Cress, A.E.; Dalkin, B.L.; Nagle, R.B. Unique expression pattern of the alpha6beta4 integrin and laminin-5 in human prostate carcinoma. *Prostate* **2001**, *46*, 240–248. [[CrossRef](#)]
29. Hynes, R.O. Integrins: Versatility, modulation, and signaling in cell adhesion. *Cell* **1992**, *3*, 11–25. [[CrossRef](#)]
30. Zhang, X.A.; Hemler, M.E. Interaction of the integrin beta1 cytoplasmic domain with ICAP-1 protein. *J. Biol. Chem.* **1999**, *274*, 11–19. [[CrossRef](#)]
31. Cheah, M.; Andrews, M.R. Integrin Activation: Implications for Axon Regeneration. *Cells* **2018**, *10*, 20. [[CrossRef](#)] [[PubMed](#)]
32. Wu, X.; Reddy, D.S. Integrins as receptor targets for neurological disorders. *Pharmacol. Ther.* **2012**, *134*, 68–81. [[CrossRef](#)] [[PubMed](#)]
33. Shattil, S.J.; Kim, C.; Ginsberg, M.H. The final steps of integrin activation: The end game. *Nat. Rev. Mol. Cell Biol.* **2010**, *11*, 288–300. [[CrossRef](#)]
34. Legate, K.R.; Wickström, S.A.; Fässler, R. Genetic and cell biological analysis of integrin outside-in signaling. *Genes Dev.* **2009**, *15*, 397–418. [[CrossRef](#)]
35. Wright, S.; Malinin, N.L.; Powell, K.A.; Yednock, T.; Rydel, R.E.; Griswold-Prenner, I. α 2 β 1 and α v β 1 Integrin Signaling Pathways Mediate Amyloid- β -Induced Neurotoxicity. *Neurobiol. Aging* **2007**, *28*, 226–237. [[CrossRef](#)] [[PubMed](#)]
36. Lim, M.; Guccione, S.; Haddix, T.; Sims, L.; Cheshier, S.; Chu, P.; Vogel, H.; Harsh, G. alpha(v)beta(3) Integrin in central nervous system tumors. *Hum. Pathol.* **2005**, *36*, 665–669. [[CrossRef](#)]
37. Matter, M.L.; Zhang, Z.; Nordstedt, C.; Ruoslahti, E. The alpha5beta1 integrin mediates elimination of amyloid-beta peptide and protects against apoptosis. *J. Cell Biol.* **1998**, *18*, 1019–1030. [[CrossRef](#)]
38. Wyssensbach, A.; Quintela, T.; Llaveró, F.; Zugaza, J.L.; Matute, C.; Alberdi, E. Amyloid β -induced astrogliosis is mediated by β 1-integrin via NADPH oxidase 2 in Alzheimer's disease. *Aging Cell* **2016**, *15*, 1140–1152. [[CrossRef](#)]
39. Alberdi, E.; Wyssensbach, A.; Alberdi, M.; Sánchez-Gómez, M.V.; Cavaliere, F.; Rodríguez, J.J.; Verkhatsky, A.; Matute, C. Ca²⁺-dependent endoplasmic reticulum stress correlates with astrogliosis in oligomeric amyloid β -treated astrocytes and in a model of Alzheimer's disease. *Aging Cell* **2013**, *12*, 292–302. [[CrossRef](#)]

40. Mroczko, B.; Groblewska, M.; Litman-Zawadzka, A.; Kornhuber, J.; Lewczuk, P. Cellular receptors of amyloid β oligomers (A β Os) in Alzheimer's disease. *Int. J. Mol. Sci.* **2018**, *19*, 1884. [[CrossRef](#)]
41. Texidó, L.; Martín-Satué, M.; Alberdi, E.; Solsona, C.; Matute, C. Amyloid β peptide oligomers directly activate NMDA receptors. *Cell Calcium* **2011**, *49*, 184–190. [[CrossRef](#)] [[PubMed](#)]
42. Ortiz-Sanz, C.; Gaminde-Blasco, A.; Valero, J.; Bakota, L.; Brandt, R.; Zugaza, J.L.; Matute, C.; Alberdi, E. Early Effects of A β Oligomers on Dendritic Spine Dynamics and Arborization in Hippocampal Neurons. *Front. Synaptic Neurosci.* **2020**, *12*, 2. [[CrossRef](#)] [[PubMed](#)]
43. Donner, L.; Gremer, L.; Ziehm, T.; Gertzen, C.G.W.; Gohlke, H.; Willbold, D.; Elvers, M. Relevance of N-terminal residues for amyloid- β binding to platelet integrin α IIb β 3, integrin outside-in signaling and amyloid- β fibril formation. *Cell. Signal.* **2018**, *50*, 121–130. [[CrossRef](#)] [[PubMed](#)]
44. Fourel, L.; Valat, A.; Faurobert, E.; Guillot, R.; Bourrin-Reynard, I.; Ren, K.; Albiges-Rizo, C. β 3 integrin-mediated spreading induced by matrix-bound BMP-2 controls Smad signaling in a stiffness-independent manner. *J. Cell Biol.* **2016**, *212*, 693–706. [[CrossRef](#)] [[PubMed](#)]
45. Fogh, B.S.; Multhaupt, H.A.B.; Couchman, J.R. Protein Kinase C, focal adhesions and the regulation of cell migration. *J. Histochem. Cytochem.* **2014**, *62*, 172–184. [[CrossRef](#)] [[PubMed](#)]
46. Ortiz-Sanz, C.; Balantzategi, U.; Quintela-López, T.; Ruiz, A.; Luchena, C.; Zuazo-Ibarra, J.; Capetillo-Zarate, E.; Matute, C.; Zugaza, J.L.; Alberdi, E. Amyloid β /PKC-dependent alterations in NMDA receptor composition are detected in early stages of Alzheimer's disease. *Cell Death Dis.* **2022**, *19*, 253. [[CrossRef](#)]
47. Müller, U.C.; Deller, T.; Korte, M. Not just amyloid: Physiological functions of the amyloid precursor protein family. *Nat. Rev. Neurosci.* **2017**, *18*, 281–298. [[CrossRef](#)]
48. Dahlgren, K.N.; Manelli, A.M.; Stine, W.B.; Baker, L.K.; Krafft, G.A.; Ladu, M.J. Oligomeric and fibrillar species of amyloid- β peptides differentially affect neuronal viability. *J. Biol. Chem.* **2002**, *277*, 32046–32053. [[CrossRef](#)]
49. Zaldua, N.; Gastineau, M.; Hoshino, M.; Lezoualc'h, F.; Zugaza, J.L. Epac signaling pathway involves STEF, a guanine nucleotide exchange factor for Rac, to regulate APP processing. *FEBS Lett.* **2007**, *22*, 5814–5818. [[CrossRef](#)]
50. Zugaza, J.L.; Lopez, M.A.; Caloca, M.J.; Dosil, M.; Movilla, N.; Bustelo, X.R. Structural Determinants for the Biological Activity of Vav Proteins. *J. Biol. Chem.* **2002**, *277*, 45377–45392. [[CrossRef](#)]
51. Mccarthy, K.D. Preparation of separate astroglial and oligodendroglial cell cultures from rat cerebral tissue. *J. Cell Biol.* **1980**, *85*, 890–902. [[CrossRef](#)] [[PubMed](#)]